Ambiguity Resolution for Permanent Scatterer Interferometry

Bert M. Kampes and Ramon F. Hanssen

***Abstract*— In the Permanent Scatterer technique of SAR interferometry there is a need for an efficient and reliable non-linear parameter inversion algorithm that includes estimation of the phase cycle ambiguities. Present techniques make use of a direct search of the solution space, treating the observations as deterministic and equally weighted, and which do not yield an exact solution. Moreover, they do not describe the quality of the estimated parameters. Here, we use the integer least-squares estimator, which has the highest probability of correct integer estimation for problems with a multivariate normal distribution. With this estimator, the propagated variance-covariance matrix of the estimated parameters can be obtained. We have adapted the LAMBDA method, part of an integer least-squares estimator developed for the ambiguity resolution of carrier phase observations in GPS, to the problem of Permanent Scatterers. Key elements of the proposed method are the introduction of pseudo-observations to regularize the system of equations, decorrelation of the ambiguities for an efficient estimation, and the combination of a bootstrap estimator with an integer least-squares search to obtain the final integer estimates. The performance of the proposed algorithm is demonstrated using simulated and real data.**

***Index Terms*— SAR Interferometry, Permanent Scatterers, non-linear parameter inversion.**

I. Introduction

In PERMANENT Scatterer (PS) interferometry time-coherent targets are analyzed in a stack of N differential interferograms (i.e., interferograms that have been corrected for the known topographic component using an external digital elevation model, DEM). All interferograms are formed relative to a single master image. An initial set of points, assumed to be potentially time-coherent, is generally obtained by a statistical analysis of the amplitude time series of the points, using the fact that points with a stable large amplitude are expected to possess a stable phase behavior too. An introduction to the PS technique is given in [1].

The phase time series of a PS point is a function of its uncompensated topographic component, its displacement, and the atmospheric delays during the acquisitions. Using the unwrapped phase differences between two nearby points and a model for the displacement, the number of parameters that needs to be estimated can be limited to $2 + D$, i.e., a height with respect to the reference DEM ("DEM error"), the mean atmospheric delay of all interferograms, and D parameters describing the displacement as a function of time. Since the atmospheric signal exhibits a power law behavior, it can be reduced considerably by taking the difference between nearby points [2]. The (line of sight) displacement for each point x can be modeled in a generic way using base functions as

$$d(t,x) = \sum_{d=1}^{D} \alpha_d(x) \cdot p_d(t), \tag{1}$$

where t is a time vector and $p_d(t)$ are arbitrary base functions with corresponding amplitudes $\alpha_d(x)$. As base functions we can use polynomials, sinusoids, etc., or even dedicated functions describing the signal of interest. In this study we use

$$p_1(t) = t, \tag{2}$$
$$p_2(t) = \sin(\tfrac{2\pi}{T}t), \tag{3}$$
$$p_3(t) = \cos(\tfrac{2\pi}{T}t), \tag{4}$$

where T is the period of the seasonal displacement, normally $T = 1$ year. With this choice of base functions, displacements can be estimated that are linear in time, and contain a superimposed seasonal displacement with certain offset t_0, since $\sin(\frac{2\pi}{T}(t-t_0) = \alpha_2 \sin(\frac{2\pi}{T}t) + \alpha_3 \cos(\frac{2\pi}{T}t)$, with $\alpha_2 = \cos(\frac{2\pi}{T}t_0)$ and $\alpha_3 = -\sin(\frac{2\pi}{T}t_0)$. This model is relatively common, see, e.g., [3] and [4].

The displacement signal Δr that is sensed at position x in interferogram i, $i = 1, \ldots, N$, is the displacement that occurred during the time between master t^0 and slave acquisition t^i

$$\Delta r_x^i = d(t^i, x) - d(t^0, x) \tag{5}$$
$$= \sum_{d=1}^{D} \alpha_d(x) \cdot (p_d(t^i) - p_d(t^0)) \tag{6}$$
$$= \sum_{d=1}^{D} \alpha_d(x) \cdot \Delta p_d(t^i) \tag{7}$$

(We thus refer to the master acquisition by $i = 0$.) Using this model for the displacement, the observed double difference wrapped phase $\phi_{x,y}^i$ denotes the difference in phase value between points x and y differenced between t^i and t^0. This can be related to the unknown parameters as

$$\phi_{x,y}^i = -2\pi \cdot a_{x,y}^i + \beta_x^i \cdot (\Delta h_y - \Delta h_x) - \frac{4\pi}{\lambda} \sum_{d=1}^{D} (\alpha_d(y) - \alpha_d(x)) \cdot \Delta p_d(t^i) + \bar{S}_{x,y} + n_{x,y}^i, \quad s.t.\ a \epsilon \mathbb{Z}, -\pi \leq \phi < \pi. \tag{8}$$

B. Kampes is with the Remote Sensing Technology Institute, German Aerospace Center, Münchner Strasse 20, 82234 Wessling, Germany; email: bert.kampes@dlr.de.

R. Hanssen is with the Delft Institute of Earth Observation and Space Systems, Delft University of Technology, Kluyverweg 1, 2629 HS Delft, The Netherlands; email: hanssen@geo.tudelft.nl

Since we consider the phase difference between two nearby points x and y (here denoted by $\{.\}_{x,y}$), the unknowns are also the differences in DEM error, displacement parameters, and bias (of atmospheric origin) between these points. The observed wrapped phase difference is unwrapped as

$$\Phi^i = \phi^i + 2\pi \cdot a^i \tag{9}$$

with integer ambiguity a^i for interferogram i. The height to phase conversion factor

$$\beta_x^i = -\frac{4\pi}{\lambda} \frac{B_{\perp x}^i}{r_x^0 \sin\theta_x^0}, \tag{10}$$

relates the DEM error, Δh, to the unwrapped phase, where λ is the wavelength, $B_{\perp x}^i$ the perpendicular baseline, r_x^0 the range to the master sensor, and θ_x^0 the local look-angle. This factor is different for each point, but mainly varies as function of the range coordinate. The atmospheric term $\bar{S}_{x,y}$ represents the mean double difference atmospheric delay between points x and y and between the master and all slave images. Although it could be assumed that the expectation values $E\{S_{x,y}^{0,i}\} = 0$ and therefore $E\{\bar{S}_{x,y}\} = 0$, in fact this expectation should be regarded as an unknown, since a large atmospheric variation in the master image could lead to a bias, and therefore to a biased estimation of the other parameters. Therefore, we write for the atmospheric delay difference in interferogram i $S_{x,y}^{i,0} = \bar{S}_{x,y} + (S_{x,y}^{i,0} - \bar{S}_{x,y})$, where $\bar{S}_{x,y} = S_{x,y}^0 - \frac{1}{N}\sum_{i=1}^N S_{x,y}^i$ and we estimate $\bar{S}_{x,y}$ assuming that $E\{S_{x,y}^{i,0} - \bar{S}_{x,y}\} = 0$. Finally, n is the noise (difference) term, with expectation 0 and variance σ^2. The noise is caused by incoherent changes of the background clutter, thermal noise, mis-registration, and atmospheric delay differences during the acquisitions. Here we focus on the optimal estimation of the integer ambiguities a^i in (9).

The basic task is to estimate the $D + N + 1$ unknown parameters ($2 + D$ real-valued parameters and $N - 1$ integer ambiguities) from the N observed wrapped phase values. Note that since it is a relative estimation, the first ambiguity does not have to be estimated, leaving $N-1$ unknown ambiguities. The solution to this problem can only be obtained by using the fact that the ambiguities are integers. For this problem, no direct inversion exists [5]. Up to now, this problem has been solved in practice by direct search methods of the parameter solution space. This means that for each unknown parameter a search grid is defined—with a certain step size and bound—and that by evaluation of the forward model a norm is computed. At the end, the solution with the minimum (or maximum) norm is used as estimate. In [1], the absolute value of the ensemble coherence γ is taken as norm

$$\gamma(\Delta h, v) = \frac{1}{N}\sum_{i=1}^{N} e^{jw^i}, \tag{11}$$

with j the imaginary unit and $w^i = \phi^i - (\beta^i \Delta h - \frac{4\pi}{\lambda} T^i \cdot v)$ the difference between observed and modeled phase. Here a linear displacement model is assumed, with velocity v.

Searching the solution space implies that a multitude of solutions for v and Δh are evaluated, yielding γ-values that are used for selecting the optimal combination. This approach is effective and quick, but with an increasing number of displacement parameters it will take more time, see [4]. More important, the method is not optimal, since (i) it depends strongly on the discretization of the solution space, (ii) it does not take into account that there are alternative solutions based on a different distribution of the ambiguities, (iii) it treats the unknown ambiguities as deterministic in stead of stochastic, and (iv) it cannot efficiently work with observations with varying variances and covariances. As a result, formal error propagation from the observations to the unknown parameters is sub-optimal.

In GPS there exists a somewhat similar problem, where the carrier phase is used to obtain a highly accurate distance measurement. The integer number of cycles however is also unknown for GPS. An efficient and optimal solution to estimate these ambiguities is given by the LAMBDA method, see [5], which is now routinely applied in GPS ambiguity resolution. Key element of the LAMBDA method is that it uses a search in the (multi-dimensional) ambiguity solution space, not in the space of the parameters of interest. Applying this integer least-squares estimator for PS ambiguity resolution has the advantage that it yields an optimal solution, capable of using any variance-covariance matrix of the observations. Besides, readily available software can be used, and computation time is practically independent of the number of displacement parameters (but only on the number of acquisitions). However, there are some distinct differences between the case of GPS and (PS) InSAR which prevent a straightforward application. The main difference is that for PS the problem is underdetermined, i.e., there are more unknowns (ambiguities plus parameters of interest) than observations (the number of interferograms), while this is not the case for GPS. Moreover, the number of ambiguities basically equals the number of satellites (images), which for GPS generally is much smaller, implying that the search takes less time. The existence of this method was already pointed out in [6], [7], and in [8], where a first simplified evaluation of a PS integer least squares estimator was performed.

II. The LAMBDA method for GPS

The Least-squares AMBiguity Decorrelation Adjustment (LAMBDA) is a method for fast GPS double difference integer ambiguity estimation. The a-priori knowledge of the integer nature of the ambiguities is used to strengthen the solution. Besides being a fast method it is also the best method in the sense that it gives the highest probability of correct integer estimation (ambiguity success rate) for problems with a multivariate normal distribution [5]. The LAMBDA method makes use of a sequential conditional least-squares search, based on transformed ambiguities. The LAMBDA method was introduced in [9] and discussed in detail in [10]. An elementary presentation of the basic principles of the method is given in [5], as well as online at http://www.geo.tudelft.nl/mgp/.

The following is a brief review of the steps involved in integer ambiguity estimation to make this paper self-contained. As a starting point, we take the (linearized) system of observation

equations

$$y = Aa + Bb + n, \tag{12}$$

where:

- y is the vector of observed minus computed measurements (double difference carrier-phase and code measurements in the case of GPS);
- a is the vector of integer-valued unknown ambiguities;
- b is the vector of real-valued unknowns for the parameters of interest. Here that are the three baseline components. Because the system of equations is linearized for GPS, this actually are increments with respect to a-priori values or the previous iteration;
- A, B are the design matrices for ambiguity terms and baseline components, respectively;
- n is the vector of measurement noise and unmodeled errors.

Since our estimation criterion will be based on the principle of least-squares, estimates for the unknown parameters of (12) follow from solving the minimization problem

$$\min_{a,b} ||y - Aa - Bb||^2_{Q_y}, \quad \text{subject to } a\epsilon\mathbb{Z}, b\epsilon\mathbb{R} \tag{13}$$

where $||.||^2_{Q_y} = (.)^* Q_y^{-1}(.)$ and Q_y is the variance-covariance matrix of the observables (the asterisk denotes the transpose). This minimization problem was referred to as integer least-squares problem in [9]. It is a constrained least-squares problem due to the integer constraint $a\epsilon\mathbb{Z}$. The solution of the integer least-squares problem will be denoted as $\check{a}$ and $\check{b}$. The solution of the corresponding unconstrained least-squares problem will be denoted as $\hat{a}$ and $\hat{b}$. The estimates $\hat{a}$ and $\hat{b}$ are referred to as the "float solution", and the estimates $\check{a}$ and $\check{b}$ as the "fixed solution".

The approach taken with the LAMBDA method, is to reparametrize the integer least-squares problem such that an equivalent problem is obtained, but one that is much easier to solve. It consists of two steps. First, an ambiguity transformation Z^* is constructed that tries to decorrelate the ambiguities. In the construction of Z^*, use is made of integer approximations to conditional least-squares transformations. The ambiguity transformation allows one to transform the original ambiguities, their least-squares estimates and their corresponding variance-covariance matrix as

$$z = Z^* a, \hat{z} = Z^* \hat{a}, Q_{\hat{z}} = Z^* Q_{\hat{a}} Z \tag{14}$$

The computation of the integer minimizers $\check{z}$ is performed in the second step of the LAMBDA method. It follows from solving

$$\min_z ||\hat{z} - z||^2_{Q_{\hat{z}}}, \; z\epsilon\mathbb{Z}. \tag{15}$$

Since matrix Z consists of integers only and is volume preserving, the obtained solution also minimizes $\hat{a} - a$ [11]. That is, the ambiguities we are interested in can be obtained by solving (15). The solution is obtained by means of a search using a set of bounds for the transformed ambiguities [12]. If the ambiguities would be totally decorrelated, the integer ambiguities would be given by means of a simple rounding of the float ambiguities, since that would minimize (15). This simple rounding scheme however does not produce the required integer least-squares estimates when matrix $Q_{\hat{z}}$ is non-diagonal. It can be shown [9] that minimizing the objective function (15) is identical to minimizing

$$\begin{aligned} \min_{z_i} \; & [(\hat{z}_1 - z_1)^2/\sigma_1^2 + (\hat{z}_{2|1} - z_2)^2/\sigma^2_{2|1} \\ & + \ldots + (\hat{z}_{n|n-1} - z_n)^2/\sigma^2_{n|n-1}], \quad z_i\epsilon\mathbb{Z} \end{aligned} \tag{16}$$

which makes use of a sequential conditional least-squares adjustment. The estimate $\hat{z}_{i|I}$ is the least-squares estimate of z_i, conditioned on $z_j, j = 1, \ldots, i-1$. In order to solve (16), a search is performed for the integer least-squares ambiguities, based on the set of bounds

$$(\hat{z}_{i|I} - z_i)^2 \leq l_i \sigma^2_{i|I} \chi^2, \quad i = 1, \ldots, n \tag{17}$$

where

$$l_i = (1 - \chi^2_{i-1}/\chi^2), \text{ with } \chi^2_{i-1} = \sum_{j=1}^{i-1} (\hat{z}_{j|J} - z_j)^2/\sigma^2_{j|J} \tag{18}$$

In order to perform the search, first a value for χ^2 needs to be determined, such that it is guaranteed that the search space contains at least one solution. Since the search takes place over the ambiguities, it will take longer when there are more ambiguities.

Once the integer least-squares vector $\check{z}$ has been found, the corresponding integer least-squares vector of the original ambiguities can be found by invoking $\check{a} = Z^{*-1}\check{z}$. These integer estimates are then used to compute the "fixed" baseline solution $\check{b}$. This can be done by inserting the estimated ambiguities in (12) and moving it to the left hand side, leaving an ordinary unconstrained least-squares problem. i.e., the observed phase values are unwrapped by $\check{y} = y - A\check{a}$, leaving

$$\check{y} = Bb + n \tag{19}$$

for which the final (unbiased) least-squares estimator for the float parameters is given by

$$\check{b} = (B^* Q_y^{-1} B)^{-1} B^* Q_y^{-1} \check{y}. \tag{20}$$

Note that matrix $Q_{\check{b}} = (B^* Q_y^{-1} B)^{-1}$ is the (full) variance-covariance matrix that describes the precision of the estimated float parameters, for example, of displacement rate and DEM error.

III. LAMBDA APPLIED TO PS INSAR

In the case of InSAR, the functional model is given by (8). In matrix notation this system of observation equations is written as

$$\begin{aligned} E\{\begin{bmatrix} \phi^1 \\ \phi^2 \\ \vdots \\ \phi^N \end{bmatrix}\} = & \begin{bmatrix} 0 & & \\ -2\pi & & \\ & -2\pi & \\ & & \ddots \end{bmatrix} \cdot \begin{bmatrix} a^2 \\ \vdots \\ a^N \end{bmatrix} \\ & + \begin{bmatrix} \beta_x^1 & \Delta p_D(1)..\Delta p_1(1) & 1 \\ \beta_x^2 & \Delta p_D(2)..\Delta p_1(2) & 1 \\ \vdots & & \\ \beta_x^N & \Delta p_D(N)..\Delta p_1(N) & 1 \end{bmatrix} \cdot \begin{bmatrix} \Delta h \\ \alpha_D \\ \vdots \\ \alpha_1 \\ \tilde{S} \end{bmatrix} \end{aligned} \tag{21}$$

$E\{.\}$ denotes expectation, and $\Delta p()$ has been defined in (7). Note that we have dropped the index $\{.\}_{x,y}$, but this system of equations still refers to the phase differences between two points. The first ambiguity is explicitly fixed to zero, since all ambiguities can be considered relative to this one. As in the case of GPS, we thus have to estimate integer ambiguities and float parameters. Unlike GPS however, it is not possible to obtain any solution without the a-priori knowledge of the integer nature of the ambiguities, due to the lack of redundancy. To solve this system of equations, additional constraints have to be introduced. As in [7], [8], we use pseudo-observations y_2 for the DEM error and each displacement parameter that is estimated that regularize the system of equations

$$E\{\begin{bmatrix} y_1 \\ y_2 \end{bmatrix}\} = \begin{bmatrix} A_1 \\ A_2 \end{bmatrix} a + \begin{bmatrix} B_1 \\ B_2 \end{bmatrix} b, \quad D\{\begin{bmatrix} y_1 \\ y_2 \end{bmatrix}\} = \begin{bmatrix} Q_{y_1} & 0 \\ 0 & Q_{y_2} \end{bmatrix}. \tag{22}$$

Matrices y_1, A_1, and B_1 are defined in (21). A_2 is a zero matrix $0_{D+1\times N-1}$, and B_2 is $[I_{D+1}, 0_{D+1\times 1}]$. The value of the pseudo-observations is normally chosen as y_2=0. Operator $D\{.\}$ denotes the dispersion of the observations. Unlike in GPS, the precision of the phase observations is not well known a-priori, since it is not guaranteed that the selected points (based on their amplitude dispersion) are actually coherent in time, and follow the displacement model that is used. In this study we assume equal variance for all observations, though in practice a variance factor can be estimated for each interferogram. The dispersion of the pseudo-observations follows from an appropriate (pessimistically chosen) a-priori standard deviation of the unknown parameters. Reasonable values are for example σ=20 meters for the DEM error, σ=20 mm/year for the linear displacement rate, and σ=10 mm for the seasonal displacement terms. This augmented system of equations can again be written symbolically similar to (12) as

$$E\{y\} = Aa + Bb, \qquad D\{y\} = Q_y. \tag{23}$$

After regularization, this system now contains the same number of unknowns as observations. This yields an exact non-redundant solution and thus the float solution for the parameters of interest will almost equal the value of the added pseudo-observations. Thus, the float solution for all parameters is extremely biased due to the introduction of the pseudo-observations. The fixed solution however is not biased, as long as the correct ambiguities were found during the search. The float solution for the ambiguities $\hat{a}$ is obtained using [13]

$$Q_{\hat{a}} = (\bar{A}^* Q_y^{-1} \bar{A})^{-1} \tag{24}$$

$$\hat{a} = Q_{\hat{a}} \bar{A}^* y \tag{25}$$

with $\bar{A} = I - B(B^* Q_y^{-1} B)^{-1} B^* Q_y^{-1}$. This solution is then transformed using (14), yielding $Q_{\hat{z}}$ and $\hat{z}$. Then, a search can be performed based on the bounds of (17), yielding the integer least-squares estimate for the ambiguities.

However, for the problem at hand, it turns out that this search can take a long time, depending on the quality and, to a lesser extent, the number of the phase observations. Therefore, we propose to also use the integer bootstrapped estimator. This estimator takes some of the correlation between the ambiguities into account, but does not search the full hyper-ellipsoid up to all bounds. It results from a sequential conditioned least-squares adjustment and it is computed as follows [12]. If N ambiguities are available, one starts with the first ambiguity $\hat{z}_1$, and rounds it to its nearest integer. Having obtained the integer value of the first ambiguity, the real-valued estimates of all remaining ambiguities are then corrected on the basis of their correlation with the first ambiguity. Subsequently, the second, now corrected, real-valued ambiguity is rounded to its nearest integer. Having obtained the value of the second ambiguity, the real-valued estimates of all remaining $N-2$ ambiguities are again corrected, but now on the basis of their correlation with the second ambiguity. This process of rounding and correcting is continued until all ambiguities are taken care of. The success rate (probability that the correct integers are estimated) for the bootstrap method can be computed as [7]

$$P(\hat{z}{=}z) = \prod_{i=1}^{n} \left[2\Phi(\frac{1}{2\sigma_{i|I}}) - 1 \right] \tag{26}$$

with

$$\Phi(x) = \int_{\infty}^{x} \tfrac{1}{\sqrt{2}} e^{-\frac{1}{2}v^2} dv \tag{27}$$

The success rate can thus be computed beforehand, based on the configuration of the acquired images in time and perpendicular baseline, and assuming a certain level of noise on the data. It is difficult to compute this probability for the LAMBDA method, but it can be shown that it outperforms the bootstrapped method, which thus can be regarded as a lower bound for it [14].

A. Computational aspects

The number of points P that need to be analyzed may be a couple of hundreds per square kilometer, particularly for city areas. And a common computation strategy is to form a large number of pairs between nearby points, for which a relative estimation has to be performed [15]. For an area of 20 by 20 kilometers, the number of points thus may be about 100000 and the number of required estimations may be 500000. If, for example, each estimation took one second, then the total computation time would come to almost 6 days. Note that a set of $P-1$ correct estimations connecting all points would be enough to compute the correct parameters at all points. The other estimations are performed only to be able to identify an incorrect estimation between points. Therefore, it is not necessary to strive for the highest possible success rate for each individual estimation between PS points. For an individual estimation, we can thus decide to not perform the integer least squares estimation (which has the highest success rate), but instead use the bootstrap estimator, or even to skip that computation completely. Note also that the position of the analyzed points follow from chance, and cannot be chosen, as, for example, in the case of GPS. This is one more reason why skipping a point does not have a big impact.

In order to increase the success rate for the bootstrap method, we run it for $k = 1, \ldots, N$ extra times, instead of

once. Each time the bootstrapped fixed ambiguity k is replaced with an integer either one higher or one lower, based on the difference between the original float value and the corrected float value. The remaining ambiguities are then computed as with the normal bootstrap method. This is similar to the search of the ambiguity solution space that is performed with the LAMBDA method, but more limited, and therefore faster. The final estimate from this extended bootstrap method is the one that has the smallest norm χ^2 according to (15). The success rate of the extended bootstrap of course is at least equal to that of (26), since the normal bootstrap is included, but it cannot be analytically quantified further.

After an estimate has been obtained using the (extended) bootstrap method, the search of the LAMBDA method is performed with the bound χ^2 from the bootstrap method. Since this search can take an extremely long time when the data contain more noise than described by the a-priori variance matrix Q_{y_1}, we discontinue it when a maximum number of ambiguities has been searched (we chose 25000 here for the maximum loop count). If the search is stopped and no candidate has been found, the estimated ambiguities that resulted from the bootstrap method are used. If a solution is obtained using the LAMBDA search, and it differs from that of the bootstrap method, the estimate is taken that has the smallest norm according to (15).

Note that if a well-fitting solution cannot be found using the bootstrapped estimation, also the search for the integer least-squares estimate takes very long. Since the time required by the (extended) bootstrap estimator does not depend on the quality of the input data, alternatively, one could try to regularize the system with several sets of randomized pseudo-observations, each time using the bootstrap estimator. Then the search to obtain the integer least-squares estimate can optionally be performed for the solution with the smallest χ^2.

Furthermore, a trivial way to speed up the computations is to use a faster computer, or to parallelize the problem on a high level, giving each processor an equal number of estimations, since each estimation can be computed independently from the others.

More importantly, a large amount of computation time can be saved by observing that the height conversion factor scales the same for all interferograms with range coordinate. This implies that we can substitute $\Delta h' = \frac{\overline{\beta}}{\beta}\Delta h$ in (8), with $\overline{\beta}$ the mean height conversion factor for the whole interferogram. After the estimation of $\Delta h'$ the correct DEM error is obtained by rescaling it with this factor. By this substitution we achieve that matrices A and B of (12) are the same for all estimations between points. This means that the transformation matrix Z only needs to be computed once, as well as the decorrelation of $Q_{\hat{a}}$, see (24), according to (14). Also, the projection matrix $(B^* Q_y^{-1} B)^{-1} B^* Q_y^{-1}$ to obtain the final float solution for the parameters of interest can be computed in advance, see (20). Finally, a faster way of unwrapping the data (then by using the matrix multiplication noted above equation 19) is to use the relation $\Phi^i = \phi^i + 2\pi \cdot a^i$ directly.

IV. Validation

In order to validate the developed combined bootstrapped/integer search estimator, and to quantify the processing time required for this algorithm, a large number of simulations are performed. The algorithm is also applied to real data, acquired by ERS-1 and -2, in order to demonstrate its capability. A total of 62 images have been processed for the Berlin area (frame 2547, track 165). The acquisition times are between May 1992 and November 2000, and the largest possible baseline between the images is 2100 meters. For the simulation, the acquisition times and perpendicular baselines are randomly selected from this configuration.

Note that both the simulated and real data results are intended to demonstrate the LAMBDA method. As stated, given a certain displacement model, several processing methods might lead to identical results. However, of all possible methods, the LAMBDA method is the one with the highest likelihood of correctly estimating the ambiguities.

A. Simulation

For the simulated data, the number of available interferograms was set to $N = 10, 11, \ldots, 60$. These N acquisition times and perpendicular baselines are randomly selected from the configuration of the real data set. For each N, the random selection of the baselines has been repeated 10 times, each time applying the retrieval algorithm 100 times. This has been done to reduce the dependency of the success rate on the actual baseline configuration, which particularly is of importance for small N. The second variable in the simulations was the amount of normally distributed noise that was added to the simulated input. The standard deviation of the noise n was set to $\sigma = 20, 30, 40, 50$ degrees. A noise level of 30° corresponds approximately to a point density of 100 points per squared kilometer (for urban areas, assuming a linear displacement model) and a noise level of 40° to 450 points, see [16]. After the addition of the noise, the simulated phase was wrapped to the interval $[-\pi, \pi\rangle$. In total thus 204 different simulation scenarios were performed, for varying N and n, where for each scenario 100 input sets were simulated. The unwrapped model phase is computed using the forward model ($\Phi = Bb$), where the parameters are randomly simulated with standard deviations $\sigma_{\Delta h}$=20 m, $\sigma_{\alpha 1}$=20 mm/y, $\sigma_{\alpha 1}$=15 mm, $\sigma_{\alpha 1}$=15 mm, and $\sigma_{\bar{S}}$=50°. The standard deviation of the pseudo-observations (Q_{y_2}) used to retrieve the input was set to $\sigma_{\Delta h}$=40 m, $\sigma_{\alpha 1}$=40 mm/y, $\sigma_{\alpha 1}$=20 mm, $\sigma_{\alpha 1}$=20 mm, and the a-priori standard deviation assumed for all interferometric phase differences (Q_{y_1}) was set to 50° in all scenarios. The base functions for the displacement model are given in (2)–(4).

Fig. 1 shows the individual CPU times required for the extended bootstrap method and for the integer least-squares search for all simulations. IDL 5.1 has been used as programming language, running on a SUN workstation utilizing a single 750 MHz UltraSPARC-III CPU. Using C or FORTRAN would likely increase the speed by a factor of (maximally) 10. The CPU times reported originate from the IDL profiler. The time for the (extended) bootstrap method is $O(N^2)$, since always N bootstraps are performed over the $N-1$ ambiguities.

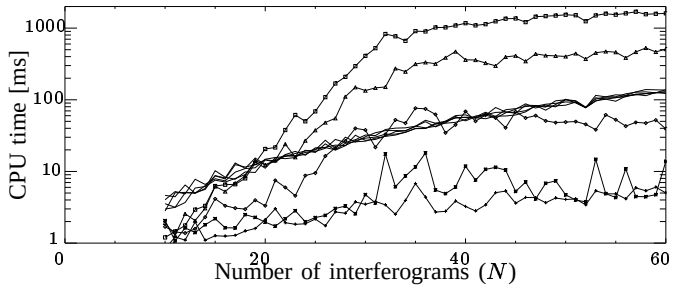

Fig. 1. CPU time required by the extended bootstrap and integer least-squares estimator as function of N and for different noise levels. The bootstrap method is represented by the bold solid lines for all noise levels; the computation time only depends on N. For the least-squares estimator the required computation time increases with increasing noise level. The lines with symbols correspond from bottom to top with a noise level of 10° (plus), 20° (asterisk), 30° (diamond), 40° (triangle), 50° (square), respectively.

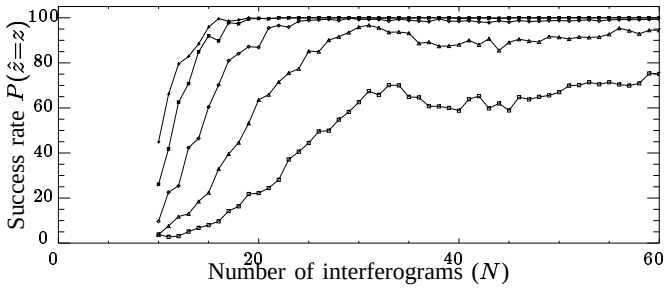

Fig. 2. Success rate of the combined bootstrap/integer least-squares method as function of N for different noise levels (from top to bottom: 10, 20, 30, 40, 50 degrees).

The time required for the integer least-squares search depends on both the quality and amount of data. For low noise levels the correct ambiguities are found extremely fast. This is caused in also by the small search bound χ^2 that is returned from the bootstrap estimator. The computation time increases with an increasing noise level. The reason is that the we search for a solution that is in correspondence with the a-priori precision, and in order to find such a solution, the bounds for the search of the hyper-ellipsoid get larger. If we would not have introduced the maximum loop count, the computation time for the least-squares search would get extremely large for noisy data, and the method would become impractical.

Fig. 2 gives an overview of the success rate for all the simulations. The individual success rate for the bootstrap and integer least-squares method is not shown, since they have to be computed both in all cases, and the combined success rate is always the highest. Only when the integer least-squares search is discontinued (using the maximum loop counter, which particularly occurs for higher noise levels), the success rate of the bootstrap method is sometimes larger than that of the integer least-squares estimator. An estimation is considered to be successful if the estimated ambiguities differ less than 1 cycle from the simulated ones (i.e., we allow the phase in 1 interferogram to be incorrectly unwrapped by 2π). The theoretic success rate has been computed with (26), but is not plotted in Fig 2. Since the a-priori standard deviation of the noise on the observations is set to 50° in all simulations, while the actual standard deviation used to simulate the noise was lower in most cases, the theoretical success rate does not correspond very well with the one obtained in practice. Also, (26) is valid for the unmodified bootstrap method, and we perform a series of slightly altered bootstraps, thus increasing the probability that the correct ambiguities are found.

It can be observed that the success rate is very high for small noise levels (up to $30°$) and more than 20 images. If there are only 10 images available, the success rate is low. This can be explained by considering that 5 float parameters and 9 integer parameters (between, say, -15 and 15) are estimated. Therefore there are simply too many possibilities that give a good fit in this case. Furthermore, it can be observed that the overall success rate increases with increasing number of images and decreasing noise level. The individual success rate of the (extended) bootstrap method was observed to be close to that of the integer least-squares search, and sometimes it was even higher (while the search theoretically has at least the same success rate). This is caused by the maximum loop count that was introduced in the least-squares search for speed considerations, causing the search to be discontinued at a certain point. This particularly occurred for larger noise levels. This also explains why the integer least-squares success rate decreases (marginally) with increasing images for equal noise level. The maximum loop count was kept constant, and thus for a smaller number of images N the hyper-ellipsoid is searched through more completely before being discontinued. However, the least-squares search is more robust (since more possible solutions are searched for), and not affected by an individual noisy value.

B. Real data

While simulations are useful to evaluate the characteristics of a retrieval algorithm under controlled circumstances, they do not necessarily incorporate all possible effects and sources of noise that are present in real data. It can happen, for example, that a certain interferogram possesses more noise than expected due to co-registration problems. In this case, the bootstrap method may not work as well as in the simulations, particularly if the ambiguities are not decorrelated very well by the applied Z-transformation. Therefore, we applied the developed algorithm also on a real data set. 1284 points have been selected over a city area (Berlin, Germany) of approximately 20 by 20 kilometer. The selected points have the lowest expected phase noise, based on their amplitude dispersion. Then, a Delaunay triangulation defined between which points the estimation was performed. The maximum distance has been limited to 2 km to reduce atmospheric influence. The total number of arcs (estimations) was 3791, and the mean distance was approximately 500 meters. The total CPU time for the estimation was 727 seconds, i.e., 0.19 seconds per estimation (using the same 750 MHz processor). Fig. 3 shows the area, the selected points, and the Delaunay network. Between the points, a DEM error, a bias, and three displacement parameters, see (2)–(4), were estimated. The a-priori interferometric phase noise for each arc was first set to 50° for all interferograms to allow for fast convergence. After an initial estimation,

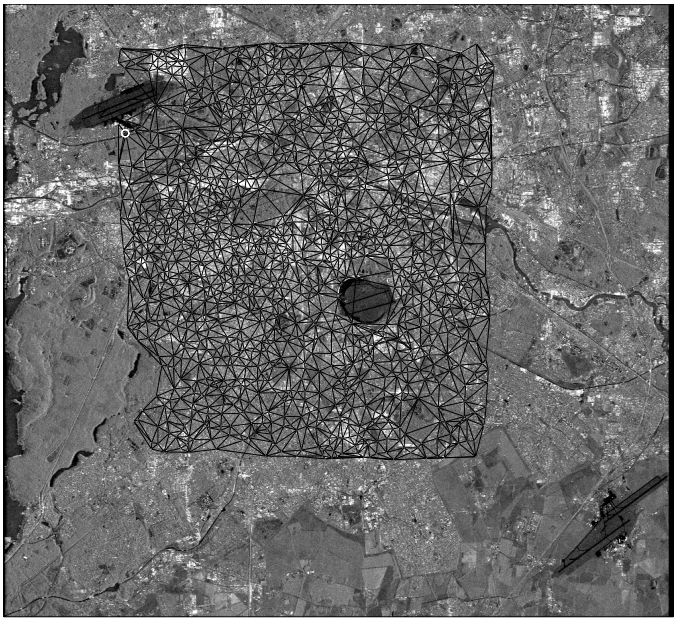

Fig. 3. Processed area. The background image shows the mean amplitude of 62 images for the Berlin area. Superimposed are the selected points and the Delaunay triangulation showing all arcs for which the parameters have been estimated. A plot of the time series is given in Fig. 6 for the arc in the upper left corner near Tegel airport, indicated by the open circle.

a variance factor per interferogram has been estimated, see [15], which was used as weight in the final estimation. The variance-covariance matrix of the estimated float parameters for this configuration of 62 acquisitions and estimated a-priori precision, according to (20), was given by

$$Q_{\check{b}} = \begin{bmatrix} 0.060 & 0.008 & -0.006 & 0.028 & -0.004 \\ 0.008 & 0.025 & 0.007 & 0.022 & 0.012 \\ -0.006 & 0.007 & 0.214 & 0.044 & 0.041 \\ 0.028 & 0.022 & 0.044 & 0.168 & 0.037 \\ -0.004 & 0.012 & 0.041 & 0.037 & 0.021 \end{bmatrix}. \quad (28)$$

The order of the parameters is DEM error, linear displacement rate, amplitude of the sinusoid term, the cosine term, and the bias of atmospheric origin, indicated in the next overview:

$\check{b}_1$	DEM error	$\sigma_{\check{b}_1}$	0.24 m
$\check{b}_2$	linear displacement	$\sigma_{\check{b}_2}$	0.16 mm/y
$\check{b}_3$	sinusoid term	$\sigma_{\check{b}_3}$	0.46 mm
$\check{b}_4$	cosine term	$\sigma_{\check{b}_4}$	0.41 mm
$\check{b}_5$	atmospheric bias	$\sigma_{\check{b}_5}$	0.14 rad

The estimations for the seasonal displacement have been transformed to a model $d(t)=A\sin(2\pi(t-t_0))$ using $t_0=\arctan(-\alpha_2/\alpha_1)/(2\pi)$ and $A=\alpha_1/\cos(2\pi t_0)$. An a-posteriori variance factor has been estimated for each arc as $\hat{\sigma}=\hat{n}^* Q_y^{-1}\hat{n}/r$ (with $\hat{n}$ the vector of least-squares residuals per arc for all interferograms, and $r=62-5$ the redundancy). Estimates for which the a-posteriori variance factor $\hat{\sigma}<2$ have been excluded from further analysis, in this case 175 estimates. Fig. 4 shows the histogram of the estimated amplitudes for the remaining 3616 estimates. Fig. 5 shows the estimated offset for reliable estimates for which $A>1$ (1571 estimates). Two peaks can be clearly identified in the

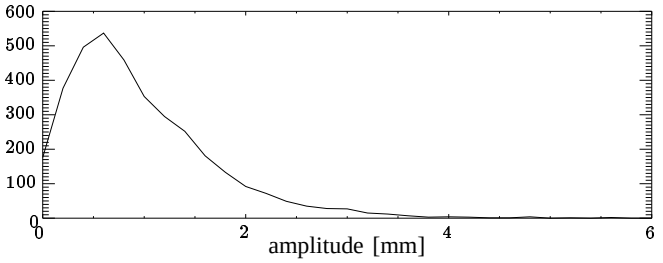

Fig. 4. Histogram of the estimated amplitude A of differential seasonal displacement for all accepted arcs.

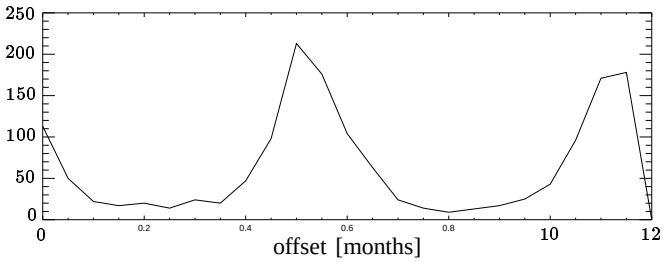

Fig. 5. Histogram of the estimated offset parameter t_0 of seasonal displacement for accepted arcs with amplitude $A > 1$.

histogram, around $t_0=5$ and $t_0=11$ months. Since in our implementation $t=0$ refers to the first acquisition, which was acquired at May 13, 1992, this means that the maximum of the seasonal displacement term for most estimates is around January 13, or June 13. If there is a correlation with temperature for the seasonal displacement, then the maximum at June 13 is more likely to be the correct one. Note that the offset has a very consistent value although it has been estimated independently for all arcs. The occurrence of two peaks can be easily explained by considering that we perform a relative estimation between two points, that is, the difference $x-y$ has an opposite sign as $y-x$.

Fig. 6 shows the time series of the interferometric phase for the arc indicated in Fig. 3. The phase differences are corrected for the estimated DEM error and linear displacement rate, and is expressed in millimeters by multiplication with $\lambda/(-4\pi)$. The maximum relative displacement lies in summer for this arc.

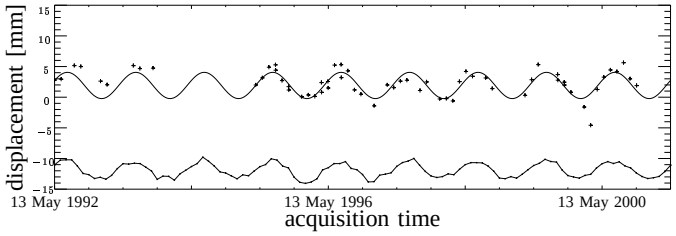

Fig. 6. Time series of the seasonal displacement phase between two nearby points, also see Fig. 3. Plotted are the spatial interferometric phase differences, converted to millimeters displacement in the line of sight, and the estimated model parameters (amplitude 2.14 mm, offset 0.94 year, i.e., maxima around June 10). A scaled version of the monthly averaged temperature is shown on the bottom for comparision (data obtained from the German Weather Services). The minimum and maximum temperatures are -3.9° and 23.7° Celcius.

The seasonal deviations from a linear displacement model are very small for the Berlin area. An alternative to retrieve the seasonal component in this case therefore could be to use the conventional ensemble coherence maximization method using a linear model, see (11), and then to estimate the seasonal component from the residual phase with respect to the linear model.

Note also that in order to obtain the displacement parameters at the points, the estimated difference parameters need to be integrated. We applied a least-squares adjustment and alternative hypothesis testing algorithm to achieve this, described in [15]. For the Berlin area no spatial pattern for the seasonal displacement was found.

V. Conclusion

The combined bootstrap and integer least-squares search method, introduced in this paper, can be applied to ambiguity resolution of interferometric data. Both an extended simulation and application on real data have demonstrated that this combination yields a good trade-off between speed and success rate. The integer least-squares method uses the a priori variance-covariance matrix of the observed phase (differences), and yields estimates with the highest probability of correct integer estimation. The developed method is efficient also when the input data are noisy due to the introduction of a maximum loop count in the integer least-squares search. Further advantages over direct search methods are that this method yields an exact solution, and the propagated variance-covariance matrix, describing the precision of the estimates.

Acknowledgment

The authors would like to thank P.J.G. Teunissen, A. Ferretti, and M. Bianchi for valuable discussions, and an anonymous reviewer for valuable comments.

References

[1] A. Ferretti, C. Prati, and F. Rocca, "Permanent scatterers in SAR interferometry," *IEEE Transactions on Geoscience and Remote Sensing*, vol. 39, no. 1, pp. 8–20, Jan. 2001.

[2] R. F. Hanssen, *Radar Interferometry: Data Interpretation and Error Analysis*. Dordrecht: Kluwer Academic Publishers, 2001.

[3] B. M. Kampes, R. F. Hanssen, and L. M. Swart, "Strategies for nonlinear deformation estimation from interferometric stacks," in *International Geoscience and Remote Sensing Symposium, Sydney, Australia, 9–13 July 2001*, 2001, pp. cdrom, 4 pages.

[4] C. Colesanti, A. Ferretti, F. Novali, C. Prati, and F. Rocca, "SAR monitoring of progressive and seasonal ground deformation using the Permanent Scatterers Technique," *IEEE Transactions on Geoscience and Remote Sensing*, vol. 41, no. 7, pp. 1685–1701, July 2003.

[5] P. J. G. Teunissen, P. J. de Jonge, and C. C. J. M. Tiberius, "A new way to fix carrier-phase ambiguities," *GPS World*, pp. 58–61, Apr. 1995.

[6] R. F. Hanssen and A. Ferretti, "Parameter estimation in PS-InSAR deformation studies using integer least-squares techniques," *EOS Trans. AGU, Fall Meet. Suppl., Abstract G62A-06*, vol. 83, no. 47, p. F37, 2002.

[7] R. F. Hanssen, P. J. G. Teunissen, and P. Joosten, "Phase ambiguity resolution for stacked radar interferometric data," in *International Symposium on Kinematic Systems in Geodesy, Geomatics and Navigation, Banff, Canada, 5–8 June 2001*, 2001, pp. 317–320.

[8] M. Bianchi, "Phase ambiguity estimation on permanent scatterers in SAR interferometry: the integer least-squares approach," Master's thesis, Politecnico di Milano/Delft University of Technology, Apr. 2003.

[9] P. J. G. Teunissen, "Least-squares estimation of the integer GPS ambiguities," in *Publications and annual report 1993*, ser. LGR-Series. Delft geodetic computing centre, Sept. 1994, no. 6, pp. 59–74.

[10] ——, "The least-squares ambiguity decorellation adjustment: a method for fast GPS integer ambiguity estimation," *Journal of Geodesy*, no. 70, pp. 65–82, 1995.

[11] P. J. G. Teunissen, P. J. de Jonge, and C. C. J. M. Tiberius, "The invertible GPS ambiguity transformation," *Manuscripta Geodaetica*, p. accepted May 9, 1994.

[12] P. J. G. Teunissen, P. J. de Jonge, and C. C. J. M. Tiberius, "The LAMBDA-method for fast GPS processing," in *GPS Technology Applications, Bucharest, Romania, Sep 26-29*, 1995.

[13] P. J. G. Teunissen, *Adjustment theory; an introduction*, 1st ed. Delft: Delft University Press, 2000.

[14] ——, "A theorem on maximizing the probability of correct integer estimation," *Artificial Satellites*, vol. 34, no. 1, pp. 3–9, 1999.

[15] B. M. Kampes and N. Adam, "Velocity field retrieval from long term coherent points in radar interferometric stacks," in *International Geoscience and Remote Sensing Symposium, Toulouse, France, 21–25 July 2003*, 2003, pp. cdrom, 4 pages.

[16] A. Ferretti, C. Prati, and F. Rocca, "Nonlinear subsidence rate estimation using permanent scatterers in differential SAR interferometry," *IEEE Transactions on Geoscience and Remote Sensing*, vol. 38, no. 5, pp. 2202–2212, Sept. 2000.

Bert Kampes was born in Woudenberg, The Netherlands, in 1974. He received the M.Sc. title in geodetic engineering from Delft University of Technology, Delft, The Netherlands, in 1998. He is currently working on the development of a scientific (radar interferometric) Permanent Scatterer system at the Remote Sensing Technology Institute of the German Aerospace Center (DLR) in Oberpfaffenhofen, Germany. He joined DLR as a scientist in 2001. From 1998 to 2001 he was employed by Delft University of Technology as an extraneous researcher. In that time he developed the Delft object-oriented radar interferometric software "Doris". His current research interests include structured software development, radar interferometry with particular focus on the utilization of large data stacks and the combination of sensors, and satellite mission design.

Ramon Hanssen (M'04) received the M.Sc. degree in geodetic engineering and the Ph.D. degree (cum laude) from Delft University of Technology, The Netherlands, in 1993 and 2001, respectively. Between 1995 and 2001 he specialized in radar remote sensing working at Delft University, the German Aerospace Center, Stanford University, Stuttgart University, and Scripps Institution of Oceanography. He is currently assistant-professor in geostatistics and radar remote sensing at the faculty of Aerospace Engineering of Delft University of Technology. His main research interests are deformation monitoring using radar interferometry, error estimation and theory, and the complementary applications of multi-sensor systems. Dr. Hanssen received the Bomford Prize of the International Association of Geodesy in 2003.